IEEE Access
Multidisciplinary | Rapid Review | Open Access Journal

Received April 9, 2019, accepted May 2, 2019, date of publication May 22, 2019, date of current version June 3, 2019.

Digital Object Identifier 10.1109/ACCESS.2019.2918179

Direct Current Injection Test Devices on Metal Cylinder: Experiment and Numerical Simulation

RUI-TAO HUANG, YAN-TAO DUAN, LI-HUA SHI, (Member, IEEE), QI ZHANG, LI-YUAN SU, AND SHI QIU

National Key Laboratory on Electromagnetic Environmental Effects and Electro-Optical Engineering, Army Engineering University of PLA, Nanjing 210007, China

Corresponding author: Yan-Tao Duan (dcmchdyt@126.com)

This work was supported by the National Key R&D Program of China under Grant 2017YFF0104300.

ABSTRACT In order to study the lightning indirect effects on the metal cylinder, the direct current injection test devices on the metal cylinder were studied in this paper based on experiment and simulation. The return conductor configuration was designed. A giant magneto resistive (GMR) sensor was calibrated to measure the intensity of the magnetic field inside and outside the metal cylinder. The impulse current injection test system similar to coaxial transmission line was established and the injection experiment was carried out. In order to verify the experimental results, a numerical simulation using the CST Microwave Studio was given. The magnetic field intensity inside and outside the metal cylinder is discussed by comparing the experimental and computational results. Moreover, the space distribution of the magnetic field is also simulated. The results show the feasibility of the test devices. The conclusions provide a foundation for further lightning indirect effect test on cylindrical ordnance.

INDEX TERMS Lightning indirect effect, direct current injection, metal cylinder, return conductor, numerical simulation.

I. INTRODUCTION

Lightning occurs average about 8 million times a day on earth, all kinds of flying objects could be struck by lightning inevitably [1]. The interaction effects of the lightning with the flying objects can be divided into direct and indirect effects. The direct effects refer to the physical damages to the flying objects including dielectric puncture, skin burn out, etc. The lightning indirect effects for flying objects represent the lightning current flowing along the discharge channel on the skin and structure of the flying objects, inducing strong electromagnetic (EM) fields [2]–[5].

Under the action of EM fields coupling effect, part of the lightning energy will be transmitted or radiated to the inside of flying objects. Meanwhile, the coupled fields will interfere electrical and electronic equipment in the flying objects. If the coupled fields exceed the immunity limits of equipment, the interference will generates damages to the equipment [6].

In common weapons and equipments, most of the flying objects are cylindrical, such as missiles, rockets shells and so on. It is provides in the Standard MIL-STD-464C [7] that the ordnance system should meet its performance requirements if the system is exposed to lightning environment or even struck by lightning. In order to test whether the system meets the requirements, we should evaluate the system according to the corresponding standards. In the standard SAE ARP5416 [8], lightning indirect effect test for small fixed wing aircraft is provided, and the test setup includes the aircraft, the current generator, a suitable return conductor and so on. The return conductors can provide reasonably uniform current distribution on the surfaces of aircraft. Referring to the method in standard SAE ARP5416, one can test the lightning indirect effect of the metal cylinder by constructing a return conductor device.

In the aspect of lightning indirect effect, many researchers have already done a lot of meaningful work. Such as Jean-Philippe Parmantier who has made a lot of achievements in studying electromagnetic models (EM models) [9]–[15]. And the models have been applied to the lightning indirect effects of aircraft. It solves many problems of cable coupling caused by lightning indirect effects. In [16], the method to build the configuration of the return conductors for aircraft was given by numerical simulation.

In the early 1990s, the direct current injection (DCI) method was introduced in the EMC test field, which is an alternative technology for testing EMC safety margin instead

The associate editor coordinating the review of this manuscript and approving it for publication was Flavia Grassi.

of HIRF [17]–[19]. Recently, we presented a method to constructing the experimental device for lightning indirect effect on the metal cylinder flying object [20]. A cage-like frame can be designed as the coupling device to carrying the impulse current injection tests. The device refers to the DCI current injection device and it adopts the typical coaxial structure of multi-line outside metal cylinder. The structure of the current injection device was determined by designing the layout of the return conductors, including the number of return conductors and the distance between the return conductor and the metal cylinder.

The main purpose of this paper is to introduce the lightning current injection test devices on the metal cylinder based on experiment and simulation. The return conductor configuration was designed. A Giant Magneto Resistive (GMR) sensor was calibrated to measure the intensity of the magnetic field. The impulse current injection test system similar to coaxial transmission line was established and the injection experiment was carried out. In order to verify the experimental results, a numerical simulation using the CST Microwave Studio was given. The magnetic field intensity inside and outside the metal cylinder are discussed by comparing the experiment and computational results. The results show the feasibility of the test devices. The conclusions provide foundation for further lightning indirect effect test on cylindrical ordnance.

II. TEST CONFIGURATION AND EXPERIMENTAL RESULTS

A. THE DESIGNED RETURN CONDUCTOR

According to the simulation analysis of [20], we designed the return conductor configuration for metal cylinder to carry out the lightning indirect effect experiment. Fig. 1 shows the simulation model. In [20], we mainly discussed the structure design of the current injection device. Uniform surface current distribution can expose electromagnetic leakage from holes and slits on the surface of metal cylinder. In order to obtain a uniform surface current distribution on metal cylinder, the structural parameters of the current injection device are determined by simulating the effects of different return conductor layouts on the surface current distribution. Fig. 2(a) shows the surface current distribution at different positions on a certain cross section of the metal cylinder under the different number (N) of return conductors. When N = 2, the uniformity of surface current distribution is poor. When N = 4, 8 and 12, the difference in uniformity of surface current distribution is small. Fig. 2(b) shows the surface current distribution at different positions on a certain cross section of the metal cylinder under the different distance (d) between return conductors and metal cylinder (N = 8). It shows that the uniformity of surface current distribution on the metal cylinder is the best when d is 50 centimeters. Based on the simulation and design results, a DCI injection device is made.

As shown in the Fig. 3, the external frame is wooden bracket, the length is 2.1 meters, the width is 1.4 meters and the height is 1.7 meters. The pulley is installed at the bottom to move. The length of coaxial return conductor arrangements

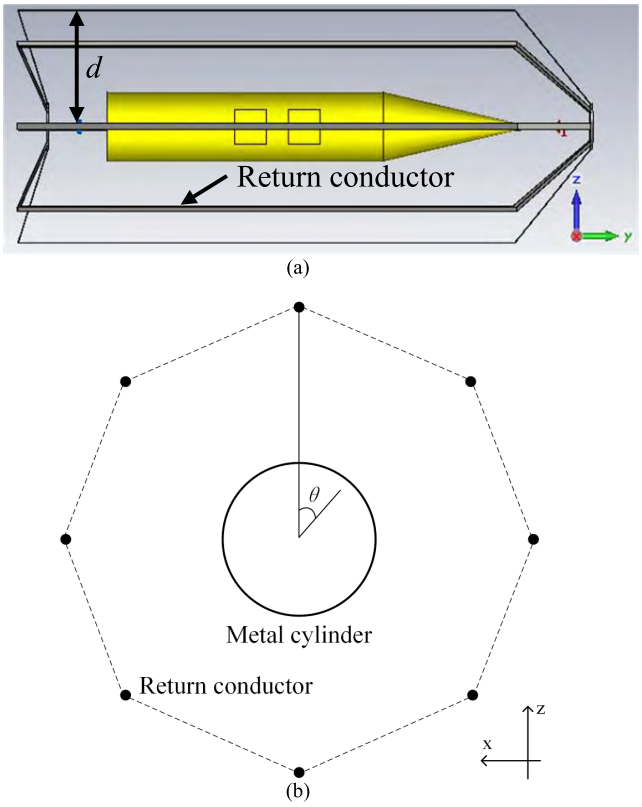

FIGURE 1. Simulation model. (a) Simulation model. (b) Angle definition.

is 3 meters and its diameter is 1 meter. The coaxial return conductor arrangements consist of 8 conductor circuits with a width of 3 cm. The eight return conductors are evenly distributed and they are fixed with 5 sets of circular insulated epoxy plates. There are two reflux rings equipped in the front and back of coaxial return conductor arrangement.

B. THE GMR SENSOR FOR MAGNETIC FIELD

In order to measure the intensity of the magnetic field inside and outside the metal cylinder, a Giant Magneto Resistive (GMR) sensor can be used [21]. The GMR sensor has an advantage of small size; it is fitted to measure some equipment with limited space, such as the missile body. The sensor has a bandwidth of about 1 MHz and it can be used to measure lightning pulse signals. In addition, the GMR probe has little effect on the magnetic field of the measured space. When the sensitive axis of the GMR sensor chip is same to the direction of the magnetic field, its output voltage varies large. We can measure the varied voltage to obtain the magnetic field intensity. Here we use a copper ring to calibrate the GMR probe, as shown in Fig. 4.

The diameter of the copper ring is 2 meters, and the GMR sensor is set in the center of it. The current flowing through the ring is I, $I = U/R$, U is the voltage across the load resistance R. The magnetic field at the center of the ring is calculated as follows [22]:

$$H(t) = \frac{I(t)}{2r} \tag{1}$$

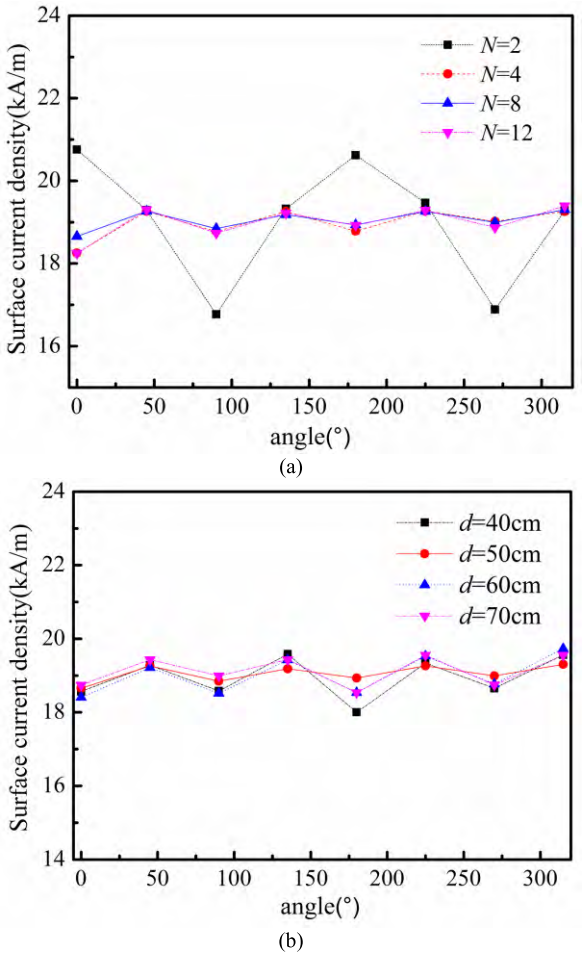

FIGURE 2. The surface current distribution on the metal cylinder. (a) Different number of return conductors. (b) Different distance between return conductor and metal cylinder

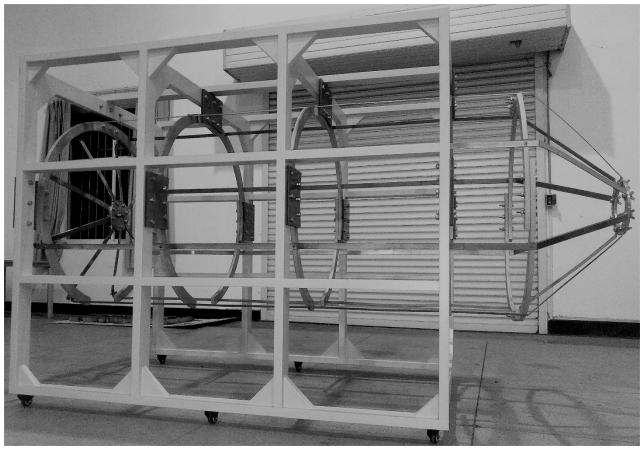

FIGURE 3. The designed return conductors for experiment.

where $I(t)$ is the current flowing through the ring, $r = 1$m is the radius of the ring. The source is generated by the impulse waveform generator of standard lightning component A [23] with lower level. The test data can be seen in Table 1. One can see that the average of calibration coefficients for X-axis measurement is 39.98 (A/m)/V.

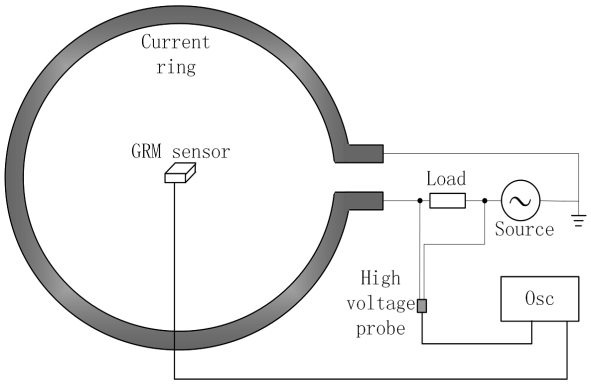

FIGURE 4. Calibration test in copper ring for GMR sensor.

TABLE 1. The data of calibration the GMR Probe for X-axis measurement.

	1	2	3	4	5
Injection current I (A)	46	53.2	62	71.2	76
Magnetic field intensity H (A/m)	23	26.6	31	35.6	38
Peak value of the measured voltage U (mV)	572	660	776	894	894
Calibration coefficient $k=H/U$ (A/m/V)	40.21	40.30	39.95	39.78	39.67
Mean of calibration coefficient (A/m/V)			39.98		

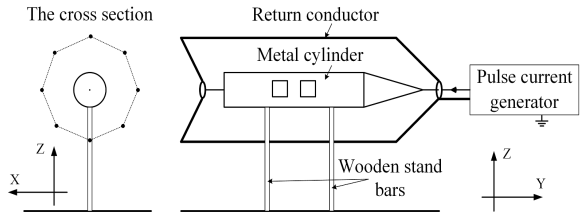

FIGURE 5. Test system connection.

The inherent noise of sensor in X-axis is about 2 mV. To improve the accuracy, minimum output level is 4 mV, that is, the lowest measurable magnetic field value is 0.15992 A/m. Since the GMR sensor uses an optical isolation system. Its maximum output voltage is 1.2 V. The highest output voltage of the optical isolation system is used as the upper limit of the measurement range of the measurement system. The highest measured magnetic field intensity in X-axis is 47.976 A/m.

C. THE IMPULSE CURRENT INJECTION TEST SYSTEM

The test system connection is shown in Fig. 5. The metal cylinder is placed in the center of the designed return conductor configuration. They form a system which is similar to coaxial transmission line. The lightning current is injected into the head of the metal cylinder; it flows from the head to the tail of metal cylinder. And it flows by the return conductor to the generator. In addition to the connection point on the end of the return conductors, the metal cylinder is insulated from the return conductors. And the whole system is insulated from the ground except the safe grounding of the generator.

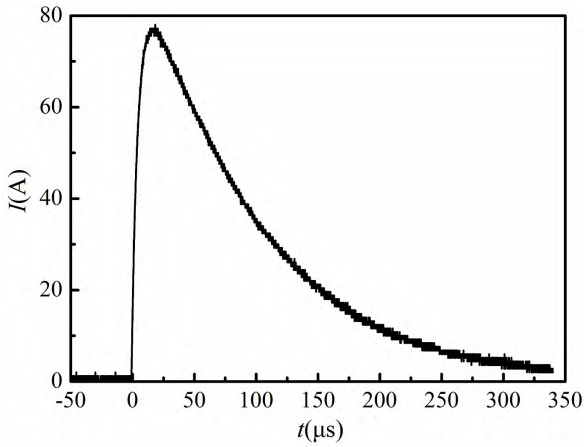

FIGURE 6. Waveform of injection current.

The injection current is the lightning current component A with a lower level, as shown in Fig. 6.

In the experiment, the test discharge current level can't reach to the 200 kA level, we use a lower level current to inject. It is generated by the impulse waveform generator of current component A, SJTU-ICG-A1.5, characterized by the rise time of 3 ± 0.5 μs, the peak time of 6.4 ± 1 μs and the full-width at half-maximum of 69 ± 5 μs. It is injected through a metal conductor that is fixed to the head of the metal cylinder. It is necessary to ensure the connection between the conductor and metal cylinder is very tight to reduce the resistance. Actually, it is strongly affected by the resistance of the whole circuit for the impulse current waveform. A Rogowski coil is used to measure the waveform of impulse current.

In the experiment, we measure the external and internal magnetic fields of the metal cylinder using the GMR sensor. The GMR sensor connects to an oscilloscope by an optical fiber transmission system. The optical receivers and oscilloscopes are placed in shielded enclosures. The coordinates are set as shown in the Fig. 5. First of all, we measure the external surface magnetic field of the metal cylinder, the GMR sensor is placed directly above the head and middle of the metal cylinder, as shown in Fig. 7(a). Then we measured the internal magnetic field of the metal cylinder, and the GMR sensor is placed inside the middle of the metal cylinder, as shown in Fig. 7(b).

D. EXPERIMENTAL RESULT

The first results are the external magnetic field above the head and middle of the metal cylinder. The typical waveform of the external magnetic field is shown in Fig. 8, and the injection current waveform is also given. One can see that the waveforms have almost the same shape. The rise times of the magnetic field waveform and the measured injection current waveform are about 9 μs and 9.48 μs, and the full-width at half-maximum is about 80 μs and 90 μs, respectively. The time rise to peak is about 16 μs.

The external magnetic field above the head of the metal cylinder is given at the different amplitudes of injection current shown in Table 2. The external magnetic field above the middle of the metal cylinder is given at the different amplitudes of injection current shown in Table 3.

In the tables, the peak value of the injection current is measured by a Rogowski coil, and the peak value of the voltage is measured by the GMR sensor, and the magnetic field is obtained by multiplying the calibration coefficients of the GMR sensor with the peak value of the measured Voltage. In the experiment, the injected current flowed from the head of the metal cylinder toward the tail, and then produced the

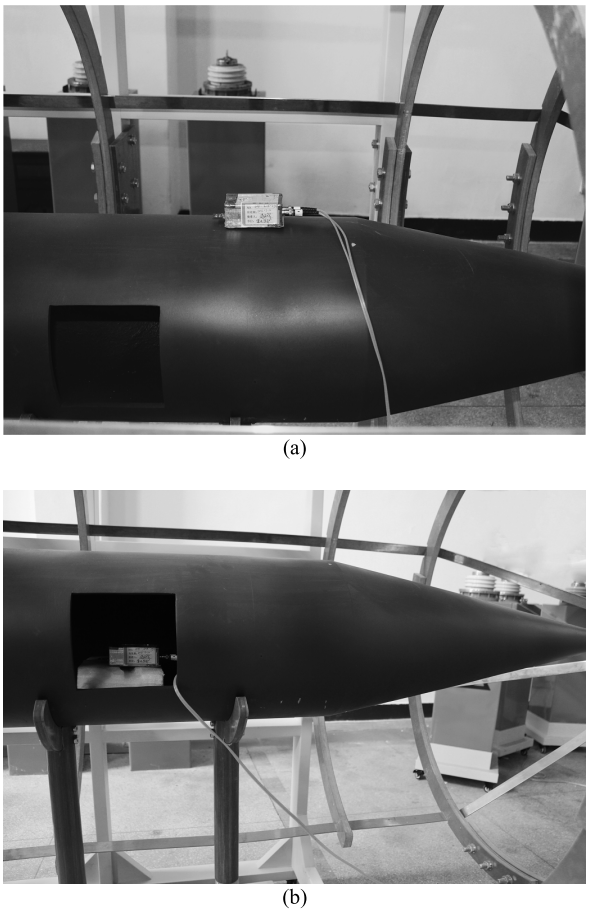

FIGURE 7. (a) and (b): Magnetic probe placed above and inside the metal cylinder.

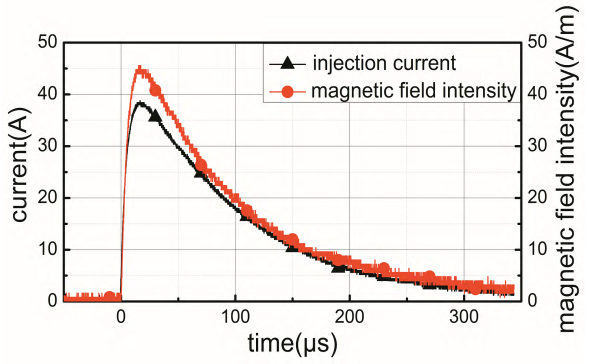

FIGURE 8. The typical waveform of the external magnetic field.

TABLE 2. The external magnetic field above the head of the metal cylinder.

	Peak value of the measured inject current (A)	Peak value of the measured Voltage(V)	Peak value of the magnetic field (A/m)
1	7.92	0.213	8.52
2	14.8	0.430	17.19
3	22.0	0.620	24.79
4	32.0	0.916	36.62
5	38.6	1.11	44.38

TABLE 3. The external magnetic field above the middle of the metal cylinder.

	Peak value of the measured inject current (A)	Peak value of the measured Voltage(V)	Peak value of the magnetic field (A/m)
1	8.72	0.146	5.84
2	15.52	0.294	11.75
3	23.8	0.496	19.83
4	31	0.684	27.35
5	39	0.916	36.62

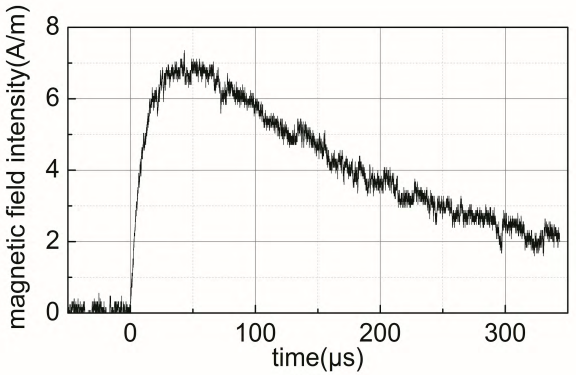

FIGURE 9. The typical waveform of the internal magnetic field.

magnetic field around it in the direction of the X-axis. So we measured the magnetic field along the X-axis only. From the tables 2, we can see that with the injection current amplitude increases, the magnetic field intensity at the measuring points increases almost linearly. However, in the tables 3, with the injection current amplitude increases, the magnetic field intensity at the measuring points increases nonlinearly. This phenomenon is mainly due to the effect of the holes on metal cylinders on the distribution of surface currents and electromagnetic fields.

The second results are the internal magnetic field inside the middle of the metal cylinder. Fig. 9 is a typical test waveform inside the metal cylinder. It can be seen that the waveform is different from the measured injection current waveform shown in Fig. 8. The rise time increases to 23 μs, and the full-width at half-maximum increases to 206 μs.

Table 4 shows the test data for the internal magnetic field inside the middle of the metal cylinder. We can see that the internal magnetic field increases almost linearly with the injection current increases. Comparing Table 4 with Table 3, the external magnetic field is forty times in comparison with the internal, if at the same level of injection current. That is to say, for better shielded metal cylinder, the coupled magnetic field inside is weak.

TABLE 4. The internal magnetic field inside the middle of the metal cylinder.

	Peak value of the measured inject current (A)	Peak value of the measured Voltage(V)	Peak value of the magnetic field (A/m)
1	147.2	0.09	3.60
2	229.6	0.13	5.20
3	306	0.177	7.08

III. SIMULATION VALIDATION

In order to verify the experimental results, a numerical simulation was given. The computational tool used in the simulation is the CST Microwave Studio. It is a powerful tool for analyzing the three-dimensional electromagnetic problems. The equal ration model of the metal cylinder is built in CST, as shown in Fig. 1. The return conductors are joined around the metal cylinder to form a cage structure. The material of the metal cylinder is aluminum, and the material of the return conductors is PEC. The diameter and thickness of the metal cylinder is 30 cm and 1cm respectively. The width and thickness of the return conductors is 3cm and 2mm respectively. The distance between return conductors and the axis of the metal cylinder is 50 cm. Lightning current component A is injected into the head of the metal cylinder and flows along the metal cylinder. Then the current flows out the metal cylinder from the tail to return conductors. They form a structure similar to the coaxial line. The end of the metal cylinder connects with terminal impedance which is set as 1 Ω to prevent resonance [9].

In the software CST, the Transmission Line Matrix (TLM) algorithm is used and the hexahedral mesh generation method is adopted. The frequency ranging between 0 and 200 MHz is accepted, and the number of mesh cells is about 2.78×10^6. In order to simulate the real flying status, open boundary conditions are adopted. To obtain the influence of lightning current flowing along the metal cylinder and its indirect effects, the total computation time should cover the half-width of the current component A. Here 350 μs is accepted.

Firstly, the magnetic probes are placed above the metal cylinder in the simulation, and the peak value of injection current is set as 39 A. The measured and simulated waveforms of the magnetic field are shown in Fig. 10 (a) and (b), respectively.

From Fig. 10 (a), it is observed that the rise time of the computed waveform and the measured waveform in are about 2.85 and 8.74 μs, respectively. The rise time of the measured waveform is longer than the computed waveform, and the maximum amplitude of the magnetic field intensity is bigger than the computed waveform and the increase of maximum amplitude is about 1.2 dB.

From Fig. 10 (b), the maximum amplitude of the measured waveform is smaller than the computed waveform and the reduction of maximum amplitude is about 0.7 dB. The rise

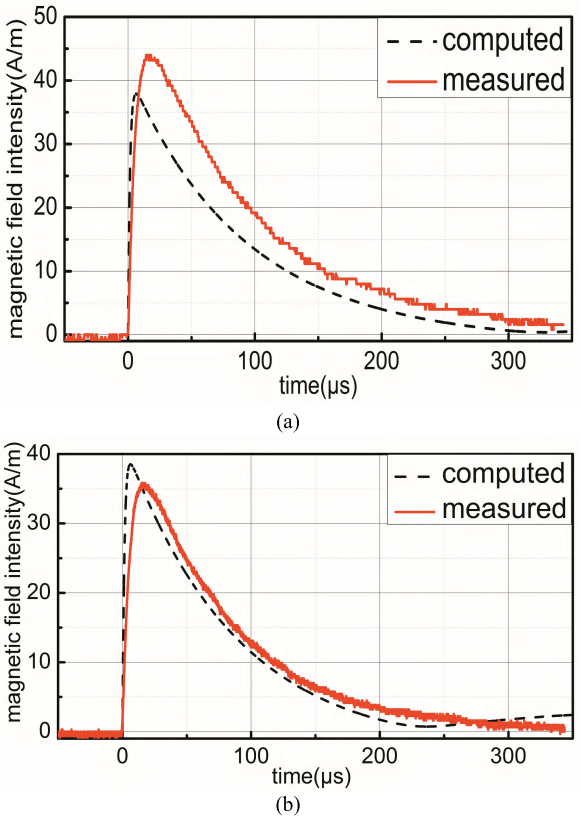

FIGURE 10. (a) and (b): The external magnetic field above the head and middle of the metal cylinder.

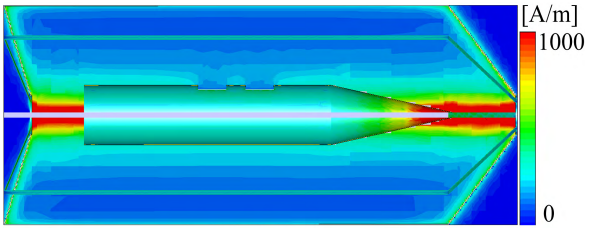

FIGURE 11. Space distribution of the magnetic field.

time of the measured waveform and the computed waveform are about 8.19 and 2.85 μs, respectively. The full-width at half-maximum of the measured waveform and the computed waveform are about 73 and 61 μs, respectively.

The discrepancies between the measured and computed magnetic field in Fig. 10 are mainly due to the fact that the test environment is not as ideal as the simulation environment, which is an uncertain factor as the welding may have great influence on the distribution of the injected current and magnetic field. Actually, with the transmission of injected current, the magnetic field intensity is weaker.

Secondly, the space distribution of the magnetic field is also simulated. Fig. 11 shows the space distribution of the external magnetic field on (x, y)-plane located at $z = 0$, when the waveform of injection current component A reaches the peak in 6.4 μs. It is obviously that the magnetic field is stronger near the lightning current path. Therefore, this may cause serious damage to sensitive equipment near the path. It is necessary to prevent the lightning current flowing inside the metal cylinder.

IV. CONCLUSION

In this paper, the lightning indirect effect test devices on metal cylinder are studied. The impulse current injection test system similar to coaxial transmission line is established to carry out the injection experiment. In order to verify the experimental results, a numerical simulation using the CST Microwave Studio is given. There are some conclusions as follows:

a. The typical waveform of the external magnetic field has almost the same shape with the injection current waveform.
b. The typical waveform of magnetic field inside the metal cylinder is different from the measured injection current waveform. The rise time is increased and the full-width at half-maximum is also increased.
c. By comparison, the external magnetic field is forty times in comparison with the internal magnetic field, if at the same level of injection current.
d. The external magnetic field appears with strong intensity in the parts with small radius of curvature and the external magnetic field shows strong intensity near the lightning current path.

The conclusions provide foundation for further lightning indirect effect test on cylindrical ordnance. In addition, to improve the simulations, one can measure the resistance of contacts in each part of the experimental structure integrated in the simulation model.

REFERENCES

[1] R. E. Orville, "Lightning physics and effects," *Atmos. Res.*, 2013.
[2] M. Apra, M. D'Amore, K. Gigliotti, M. S. Sarto, and V. Volpi, "Lightning indirect effects certification of a transport aircraft by numerical simulation," *IEEE Trans. Electromagn. Compat.*, vol. 50, no. 3, pp. 513–523, Aug. 2008.
[3] K. R. Umashankar, A. Taflove, and B. Beker, "Calculation and experimental validation of induced currents on coupled wires in an arbitrary shaped cavity," *IEEE Trans. Antennas Propag.*, vol. 35, no. 11, pp. 1248–1257, Nov. 1987.
[4] C. Guiffaut and A. Reineix, "Cartesian shift thin wire formalism in the FDTD method with multiwire junctions," *IEEE Trans. Antennas Propag.* vol. 58, no. 8, pp. 2658–2665, Aug. 2010.
[5] C. Holloway, M. S. Sarto, and M. Johansson, "Analyzing carbon-fiber composite materials with equivalent-layer models," *IEEE Trans. Electromagn. Compat.*, vol. 47, no. 4, pp. 833–844, Nov. 2005.
[6] B. Zhou, L. Shi, and C. Gao, *Electromagnetic Protection of National Defense Engineering*. Beijing, China: National Defense Industry Press, 2005.
[7] *Electromagnetic Environmental Effects Requirements for Systems*. Standard MIL-STD-464C, Dec. 2010.
[8] *Aircraft Lightning Test Methods*, Standard SAE-ARP5416, 2005.
[9] J.-P. Parmantier, "First realistic simulation of effects of EM coupling in commercial aircraft wiring," *Comput. Control Eng. J.*, vol. 9, no. 2, pp. 52–56, Apr. 1998.
[10] L. Paletta, J. P. Parmantier, F. Issac, P. Dumas, and J. C. Alliot, "Susceptibility analysis of wiring in a complex system combining a 3-D solver and a transmission-line network simulation," *IEEE Trans. Electromagn. Compat.*, vol. 44, no. 2, pp. 309–317, May 2002.
[11] J. P. Parmantier, "Numerical coupling models for complex systems and results," *IEEE Trans. Electromagn. Compat.*, vol. 46, no. 3, pp. 359–367, Aug. 2004.

[12] G. Andrieu, A. Reineix, X. Bunlon, J. Parmantier, L. KonÉ, and B. DÉmoulin, "Extension of the "equivalent cable bundle method" for modeling electromagnetic emissions of complex cable bundles," *IEEE Trans. Electromagn. Compat.*, vol. 51, no. 1, pp. 108–118, Feb. 2009.
[13] J. P. Parmantier, F. Issac, and V. Gobin, "Indirect effects of lightning on aircraft and rotorcraft," *AerospaceLab*, pp. 1–27, 2015.
[14] D. Prost, F. Issac, T. Volpert, W. Quenum, and J. Parmantier,, "Lightning-induced current simulation using RL equivalent circuit: Application to an aircraft subsystem design," *IEEE Trans. Electromagn. Compat.*, vol. 55, no. 2, pp. 378–384, Apr. 2013.
[15] J. P. Parmantier *et al.*, "Distributed voltage sources on transmission-lines—Unified low frequency model," in *Proc. Int. Symp. Electromagn. Compat.-EMC EUROPE*, Sep. 2017, pp. 1–6.
[16] L. Su, C. Gao, Y. Duan, and F. Guo, "Simulation research on the return conductor configuration of aircraft lightning indirect effect test," *Int. J. Appl. Electromagn. Mech.*, vol. 53, no. 3, pp. 487–496, 2017.
[17] A. M. Wellington, "Direct current injection as a method of simulating high intensity radiated fields (HIRF)," in *Proc. IEE Colloq. EMC Test. Conducted Mech.*, May 1996, pp. 4-1–4-6.
[18] N. J. Carter and P. E. Willis, "EMC testing of high-integrity digital systems in aircraft," in *Proc. IEE Colloq. EMC High Integrity Digital Syst.*, May 1991, pp. 4-1–4-9.
[19] X. Lu, G. Wei, X. Pan, X. Zhou, and L. Fan,, "A pulsed differential-mode current injection method for electromagnetic pulse field susceptibility assessment of antenna systems," *IEEE Trans. Electromagn. Compat.*, vol. 57, no. 6, pp. 1435–1446, Dec. 2015.
[20] R. Huang, Y. Duan, K. Luo, and L. Shi, "Simulation research on the return conductor configuration for lightning indirect effect test of metal cylinder," in *Proc. IEEE 5th Int. Symp. Electromagn. Compat. (EMC-Beijing)*, Beijing, China, Oct. 2017, pp. 494–497.
[21] B. Zhou, Y. Ding, and T. Wang, "Measurement of lightning surface current on the conductor," *J. PLA Univ. Sci. Technol. Natural Sci. Ed.*, vol. 14, no. 5, pp. 484–489, 2013.
[22] BS Guru, HR Hiziroglu. *Electromagnetic Field Theory Fundamentals*. Beijing, China: China Machine Press, 2005.
[23] *Aircraft Lightning Environment and Related Test Waveforms*, Standards SAE-ARP5412B, 2013.

RUI-TAO HUANG was born in Hebei, China, in 1994. He received the B.S. degree from the Nanjing University of Science and Technology, Nanjing, China, in 2016. He is currently pursuing the M.S. degree with the Army Engineering University of PLA. His research interests include computational electromagnetics and EMP.

YAN-TAO DUAN was born in Hebei, China, in 1980. He received the B.S., M.S., and Ph.D. degrees in electric systems and automation from the Nanjing Engineering Institute, Nanjing, China, in 2002, 2006, and 2010, respectively. He is currently an Associate Professor with the National Key Laboratory on Electromagnetic Environmental Effects and Electro-optical Engineering, Army Engineering University of PLA, Nanjing, China. His research interests include computational electromagnetics and EMP.

LI-HUA SHI (M'96) was born in Hebei, China, in 1969. He received the B.S. degree from Xidian University, Xi'an, China, in 1990, and the Ph.D. degree from the Nanjing University of Aeronautics and Astronautics, Nanjing, China, in 1996. He is currently a Professor and the Director of the National Key Laboratory on Electromagnetic Environmental Effects and Electro-Optical Engineering, Army Engineering University of PLA, Nanjing, with a focus on time-domain measurement and signal processing technology. He is a member of the IEEE EMC Society and an HEMP Fellow of the Summa Foundation, USA.

QI ZHANG was born in Shandong, China, in 1987. He received the B.S. degree from Guangxi University, Nanning, China, in 2009, and the M.S. and Ph.D. degrees from the PLA University of Science and Technology, Nanjing, in 2012 and 2015, respectively. He is currently a Lecturer with the National Key Laboratory on Electromagnetic Environmental Effects and Electro-Optical Engineering, Army Engineering University of PLA, Nanjing. His research interests include lightning protection and computational electromagnetics.

LI-YUAN SU was born in 1978. She received the Ph.D. degree from the Army Engineering University of PLA, where she is currently a Lecturer with the National Key Laboratory on Electromagnetic Environmental Effects and Electro-Optical Engineering. Her current research interests include electromagnetic protection and EMC.

SHI QIU was born in Shandong, China, in 1984. He received the B.S. and Ph.D. degrees from the PLA University of Science and Technology, Nanjing, China, in 2005 and 2012, respectively. He is currently an Associate Professor with the National Key Laboratory on Electromagnetic Environmental Effects and Electro-Optical Engineering, Army Engineering University of PLA. His research interests include lightning physics and lightning protection.